Neoplasia 67 (2025) 101204

Contents lists available at ScienceDirect

Neoplasia

journal homepage: www.elsevier.com/locate/neo

Original Research

SKI regulates rRNA transcription and pericentromeric heterochromatin to ensure centromere integrity and genome stability

Víctor Pola-Véliz [a,e,f,g,h], David Carrero [a], Eduardo A. Sagredo [a,i], Víctor Inostroza [a], Claudio Cappelli [a,j], Solange Rivas [a], Mirit Bitrán [a], Evelyn Zambrano [a,b], Evelin Gonzalez [c], Fernanda Morales [a,b], Marcia Manterola [a,d], Martín Montecino [e,f,g,h], Ricardo Armisén [c], Katherine Marcelain [a,b,*]

[a] Departamento de Oncología Básico Clínico, Facultad de Medicina, Universidad de Chile, Santiago, Chile
[b] Centro para la prevención y el control del Cáncer (CECAN), Facultad de Medicina, Universidad de Chile, Santiago, Chile
[c] Centro de Genética y Genómica, Instituto de Ciencias e Innovación en Medicina, Facultad de Medicina, Clínica Alemana Universidad del Desarrollo, Santiago, Chile
[d] Center for Translational Studies in Stress and Mental Health (C-ESTRES), Universidad de Valparaíso, Valparaíso, Chile
[e] Institute of Biomedical Sciences, Faculty of Medicine, Universidad Andrés Bello
[f] Millennium Nucleus of Neuroepigenetics and Plasticity
[g] Center for Biomedical Research, Faculty of Medicine, Universidad Andrés Bello, Santiago, Chile
[h] FONDAP Center for Genome Regulation, Faculty of Biological Sciences, Universidad Andrés Bello, Santiago, Chile
[i] Current Address: Science for Life Laboratory, Department of Microbiology, Tumor and Cell Biology, Karolinska Institutet, 171 65 Solna, Sweden
[j] Current Address: Laboratorio de Inmunoepigenética. Instituto de Bioquímica y Microbiología, Facultad de Ciencias, Universidad Austral de Chile, Valdivia, Chile

ARTICLE INFO

Keywords:
SKI
rRNA
Pericentromeric heterochromatin
Chromosomal Instability
Breast cancer

ABSTRACT

Accurate chromosome segregation and ribosomal gene expression silencing are essential for maintaining genome integrity, and disruptions in these processes are key for oncogenesis and cancer progression. Here, we demonstrate a novel role for the transcriptional co-repressor SKI in regulating rDNA and pericentromeric heterochromatin (PCH) silencing in human cells. We found that SKI localizes to the rDNA promoter on acrocentric chromosomes and is crucial for maintaining H3K9 trimethylation (H3K9me3) and repressing 45S rRNA gene expression. SKI is also associated with BSR and HSATII satellites within PCH, where is necessary for H3K9 methylation and recruitment of SUV39H1 and HP1α, key players for heterochromatin silencing and centromere function. Consequently, SKI deficiency disrupted centromere integrity and resulted in aberrant chromosome segregation, micronuclei formation, and chromosome instability. The identification of SKI as a key participant in the epigenetic-mediated silencing of pericentromeric and ribosomal DNA provides a fundamental insight, paving the way for new research into the intricate relationship between transcriptional regulation and genome instability during cancer progression, and opening novel opportunities for therapeutic intervention.

Introduction

Maintaining genome integrity during mitosis is crucial for accurate transmission of genetic information. Errors in chromosome segregation can lead to aneuploidy and chromosomal instability (CIN), both of which contribute to tumor progression, poor clinical outcomes, and therapy resistance [1].

The centromere is essential for faithful chromosome segregation [2]. In human, centromeric regions primarily comprise alpha satellite DNA, a ~171-bp repeat organized into tandem arrays containing CENP-A nucleosomes that facilitate kinetochore assembly [3,4]. Centromeres are flanked by transcriptionally silenced pericentromeric heterochromatin (PCH). Proper assembly and maintenance of centromeric and pericentromeric chromatin are critical for centromere structural integrity and sister chromatid cohesion, ensuring accurate chromosome segregation and genomic stability [5,6].

Pericentromeric regions contain several repetitive, non-conserved DNA sequences, including β-satellite (BSR), γ-satellite, and Human Satellite (HSAT) I, II, and III [7,8]. Despite interspecies DNA sequence variations, the fundamental architecture and function of centromeric

* Corresponding author at: Av. Las Palmeras 299. Departamento de Oncología Básico Clínico, Campus Occidente Facultad de Medicina, Santiago, Chile.
E-mail address: kmarcelain@uchile.cl (K. Marcelain).

https://doi.org/10.1016/j.neo.2025.101204
Received 26 March 2025; Accepted 23 June 2025
Available online 2 July 2025

and pericentromeric chromatin are highly conserved, driven primarily by the epigenetic organization of chromatin [9].

PCH is epigenetically characterized by histone H3 lysine 9 trimethylation (H3K9me3), histone hypoacetylation, and extensive DNA methylation. H3K9me3-enriched nucleosomes serve as docking sites for heterochromatin protein 1 (HP1) isoforms (HP1α, HP1β, and HP1γ), which recruit the histone methyltransferases SUV39H1 and SUV39H2, promoting H3K9me3 establishment and propagation [10,11]. While the roles of SUV39H1 and HP1 in H3K9me3 establishment and spreading are well established, other factors maintaining PCH's epigenetic state are less understood. Pharmacological inhibition of histone deacetylases (HDACs) and DNA methyltransferase 1 (DNMT1) disrupts PCH integrity, leading to impaired chromosome condensation, missegregation, rearrangements, micronuclei formation, and tumorigenesis [12]. On the other hand, the transcriptional co-repressor SKI localizes to PCH in murine embryonic fibroblasts (MEFs) and is required for H3K9 trimethylation and silencing of nearby genes [13]. SKI binds to transcription factors, recruiting co-repressors like HDACs, NCoR, and mSin3A to gene promoters [14–16]. SKI exhibits both pro- and anti-oncogenic activities, with evidence supporting its role as a tumor suppressor in various human cancers, including breast cancer [14,17–19]. Furthermore, Ski-null MEFs display high levels of aneuploidy and CIN, and SKI loss of function may increase tumor susceptibility [14,20,21].

Impaired PCH maintenance is implicated in cancer progression and CIN [22–26]. In breast cancer, pericentromeric DNA hypomethylation and altered H3K9me3 patterns correlate with aggressive carcinomas and a CIN phenotype [22,24,26]. These findings suggest that PCH disruption is a key driver of malignancy, and targeting PCH may offer a therapeutic strategy in breast cancer.

Here, we uncover, for the first time, the role of SKI in regulating the

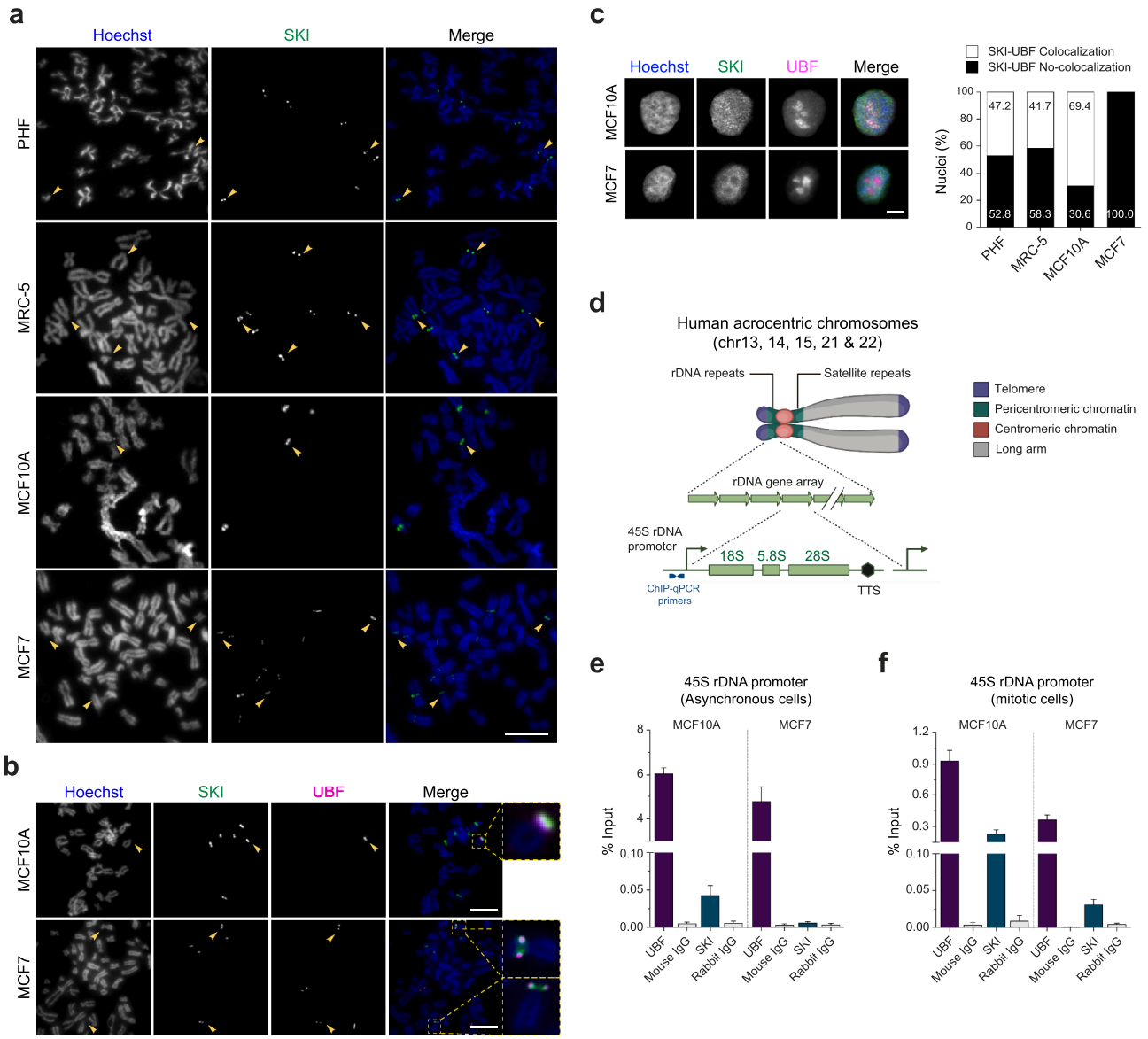

Fig. 1. Association of SKI with acrocentric chromosomes and rDNA in human cells. (a) SKI immunodetection on chromosome spreads. Representative images show SKI localization on chromosome spreads from PHF (primary fibroblasts), MRC-5 (non-transformed immortalized fibroblasts), MCF10A (non-transformed immortalized epithelial breast cells), and MCF7 (breast tumor-derived) cell lines. (b) Colocalization of SKI and UBF on mitotic chromosomes. Yellow arrowheads indicate acrocentric chromosomes positive for the SKI signal. (c) Examples of distinct patterns of Ski staining in interphase nuclei (left) and distribution of nuclei based on SKI/UBF colocalization (n = 180 nuclei per cell line, three independent experiments). Scale bar= 2 μm. (d) Schematic representation of human mitotic acrocentric chromosomes showing the location of primers for ChIP-qPCR assays in a single rDNA repeat (blue arrows). (e-f) SKI and UBF enrichment on rDNA promoter. ChIP assays using antibodies against SKI and UBF were performed to assess enrichment on the rDNA promoter in asynchronous and mitotic MCF10A and MCF7 cell lines. Results are expressed as % of Input ± SEM. Normal IgG served as a specificity control.

H3K9me3/acetylation landscape of PCH and maintaining genome stability in breast cancer.

Results

SKI associates with the rDNA promoter on human acrocentric chromosomes

We previously demonstrated SKI's association with pericentromeric chromatin in mitotic murine fibroblasts [13]. Intriguingly, this localization has not been described in human cells. To investigate SKI localization in human cells, we performed immunofluorescence on metaphase chromosome spreads from primary human fibroblasts (PHF), immortalized fibroblasts (MRC-5), breast epithelial (MCF10A), and breast cancer (MCF7) cell lines (Fig. 1a). SKI localizes near the centromeric regions of several chromosomes, including some with an acrocentric morphology.

Ribosomal DNA (rDNA) tandem repeats are in nucleolus organizer regions (NORs) and, during mitosis, are packaged into the pericentromeric regions of acrocentric chromosomes. To explore a potential association of SKI with NORs, we examined the mitotic distribution of SKI, using UBF (the transcription factor that activates rDNA repeats), as a marker for active NORs (Fig. 1b). In MCF10A and MCF7 cells, SKI co-localized with UBF near the centromeres of a subset of metaphase chromosomes. However, in interphase nuclei, MCF7 cells exhibited a significantly lower percentage of SKI-UBF co-localization compared to primary fibroblasts, MRC-5, and MCF10A cells (Fig. 1c).

ChIP-qPCR assays show a high enrichment of UBF in the 45S rDNA promoter in asynchronous as well as mitotic MCF10A and MCF7 cells. A lower but significant occupancy of SKI in this region was also detected in asynchronous and mitotic MCF10A but as expected, only in mitotic MCF-7 cells (Fig. 1d-f).

SKI-dependent epigenetic regulation of rDNA expression

In cycling cells, the mitotic assembly of rDNA transcription machinery determines the expression of rDNA repeats at the next interphase [27,28]. Thus, we evaluated whether SKI regulates the expression of rDNA genes. Since MCF10A expresses higher levels of SKI protein and mRNA than MCF7, we used shRNAs to knock down the expression of SKI by more than 50 % in MCF10A, and retroviral transduction to overexpress the protein in MCF7. These strategies did not affect UBF protein levels (Fig. 2a and S2). Knockdown significantly decreased the occupancy of SKI on rDNA promoter in mitotic MCF10A cells. Conversely, overexpression of the protein significantly increased the occupancy on the rDNA promoter in +*SKI* MCF7 cells (Fig. 2b). No differences between wild type (WT) and their respective controls (shScramble -shCtr- and mock) were observed.

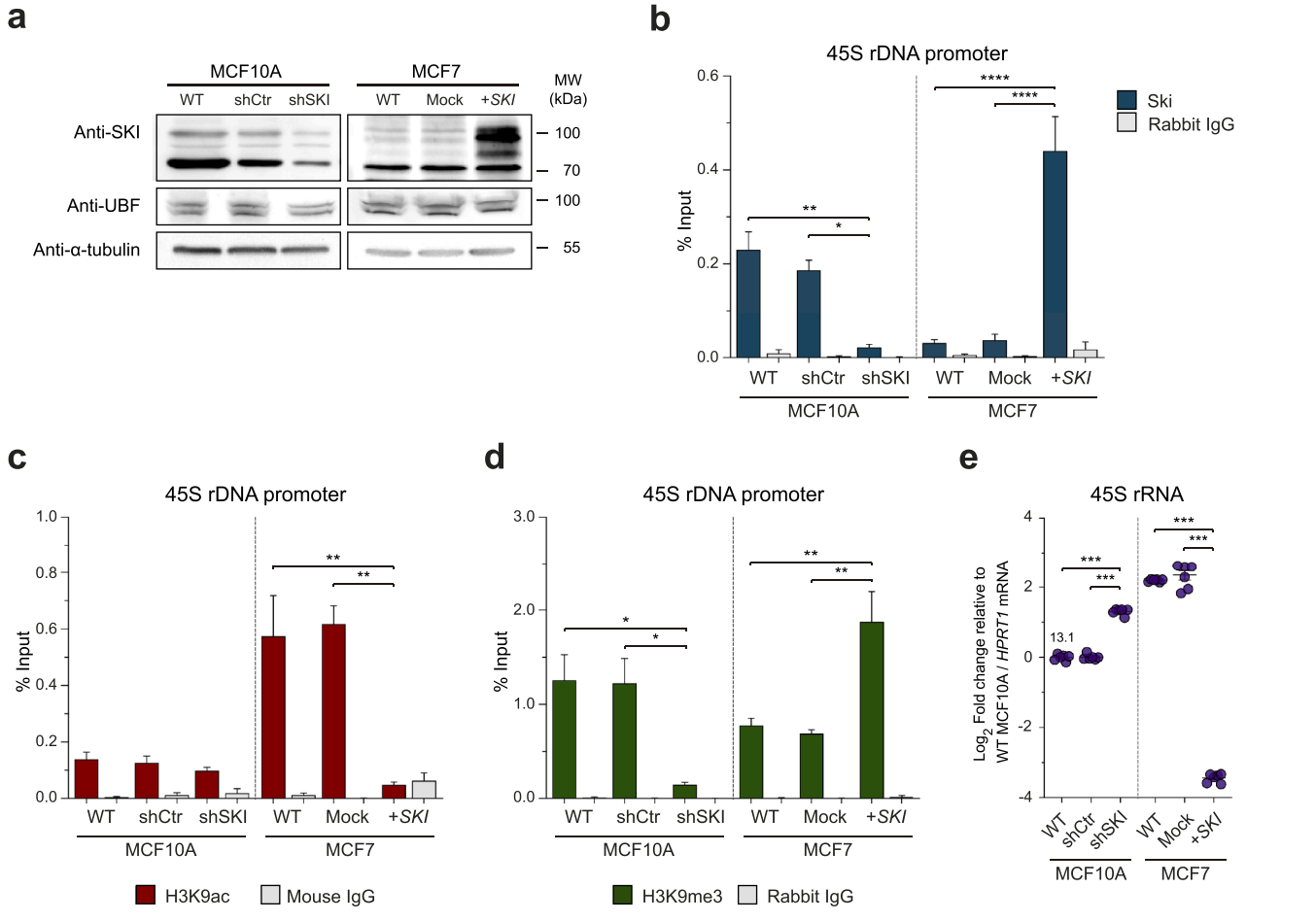

Fig. 2. SKI-dependent H3K9 Acetylation and Methylation at the rDNA Promoter during Mitosis impact 45S rRNA Expression. (a) MCF10A cells were transduced with lentiviral particles expressing either a SKI-targeting shRNA (shSKI) or a non-targeting control shRNA (shCtr). MCF7 cells were transduced with retroviral particles expressing either human SKI cDNA (+SKI) or an empty vector control (Mock). Western blot analysis confirmed SKI and UBF protein levels; α-tubulin served as a loading control. (b-d) ChIP assays were performed using antibodies against SKI (b), H3K9 acetylation (H3K9ac) (c), and H3K9 trimethylation (H3K9me3) (d) in mitotic MCF10A and MCF7 cells. ChIP enrichment is expressed as the percentage of input ± SEM. Normal IgG served as a specificity control. (e) Relative 45S rRNA levels were measured by RT-qPCR in MCF10A and MCF7 cells. Statistical analysis was performed using one-way ANOVA with multiple comparisons. Significance levels are indicated by asterisks: *p < 0.05, **p < 0.01, ***p ≤ 0.001, ****p < 0.0001.

Levels of H3K9ac are low at the rDNA promoters in control MCF10A cells, and SKI knockdown did not affect these levels. However, a dramatic decrease was induced by SKI overexpression in MCF7 (Fig. 2c). In the opposite way, H3K9me3 enrichment significantly decreased after SKI knockdown in MCF10A, and increased upon overexpression in MCF7 mitotic cells (Fig. 2d). These epigenetic changes affect the expression of rDNA. shSKI MCF10A cells increased about 2.5 times the expression of the 45S ribosomal gene compared to WT and shCtr cells, while Ski overexpression dramatically reduced its expression in MCF7 cells (Fig. 2e).

Overall, these results indicate that Ski deposition on the rDNA promoter during mitosis can maintain the H3K9me3 status of chromatin, repressing the expression of the 45S gene in breast epithelial cells.

SKI is essential for pericentric heterochromatin and centromere integrity

To further assess whether Ski's effect on rDNA extends to PCH in acrocentric chromosomes, we designed chromosome-specific primers for BSR and HSATII repeats at chr15 and chr22, respectively (Fig. 3a and b). Our results indicated that the anti-Ski antibody successfully immunoprecipitated the BSR and HSATII sequences in WT and shCtr MCF10A during mitosis. SKI knockdown resulted in a decrease in the immunoprecipitation of these sequences, similar to the negative control (Fig. 3c). In mitotic MCF7 cells, significant occupancy on BSR and HSATII was observed only in Ski-overexpressing cells. The endogenous levels of SKI in WT and Mock MCF7 did not precipitate these sequences (Fig. 3d).

SKI knockdown resulted in an overall increased level of H3K9ac and decreased H3K9me2/H3K9me3 in mitotic MCF10A cells (Fig. 4a, left). On the other hand, overexpression of SKI reduced levels of H3K9ac and increased H3K9me2/H3K9me3 levels in mitotic MCF7 cells (Fig. 4a, right). Next, we evaluated whether SKI occupancy modulates epigenetic changes in pericentromeric satellite repeats. Downregulation of *SKI* expression results in increased H3K9ac and reduced H3K9me3 of BSR and HSATII in MCF10A (Fig. 4b-c). Conversely, a reduction of H3K9ac and increased H3K9me3 in BSR and HSATII were induced upon ectopic expression of *SKI* in MCF7 cells (Fig. 4d-e).

As SUV39H1 and HP1 are critical for establishing and propagating heterochromatin at pericentromeric regions [12], we sought to determine if SKI-mediated H3K9me3 modulated the recruitment of SUV39H1 and HP1α to BSR and HSATII. We observed a marked reduction in SUV39H1 and HP1α accumulation at satellite repeats in SKI-depleted mitotic cells (Fig. 5a-c). Subsequently, we explored whether these SKI deficiency-induced changes in heterochromatin protein composition affected centromere architecture. Although total CENP-A protein levels remained unchanged upon SKI knockdown (Fig. S4), we found a significant decrease in both the CENP-A signal and its incorporation into centromeric nucleosomes, as demonstrated by diminished enrichment at α-satellite sequences (Fig. 5c-d).

Therefore, SKIs localization in PCH maintains the repressive heterochromatin marks required for proper centromere formation.

SKI depletion leads to aberrant chromosome segregation, aneuploidy and chromosomal instability (CIN)

We examined anaphase events to determine whether the observed pericentromeric heterochromatin (PCH) and centromere structural defects in SKI-deficient cells impact chromosome segregation. Microscopic analysis of shSKI MCF10A cells revealed two prominent aberrations: multipolar metaphases and chromatin bridges (Fig. 6a). Furthermore, SKI deficiency resulted in micronuclei formation in over 20 % of cells (Fig. 6b) and subsequent aneuploidy in 80 % of cells (Fig. 6c-f). Reducing SKI also impacts the length of deletions, which increase as cells go through more divisions (passages) (Fig. 6g). These findings demonstrate that the loss of SKI expression leads to aneuploidy and

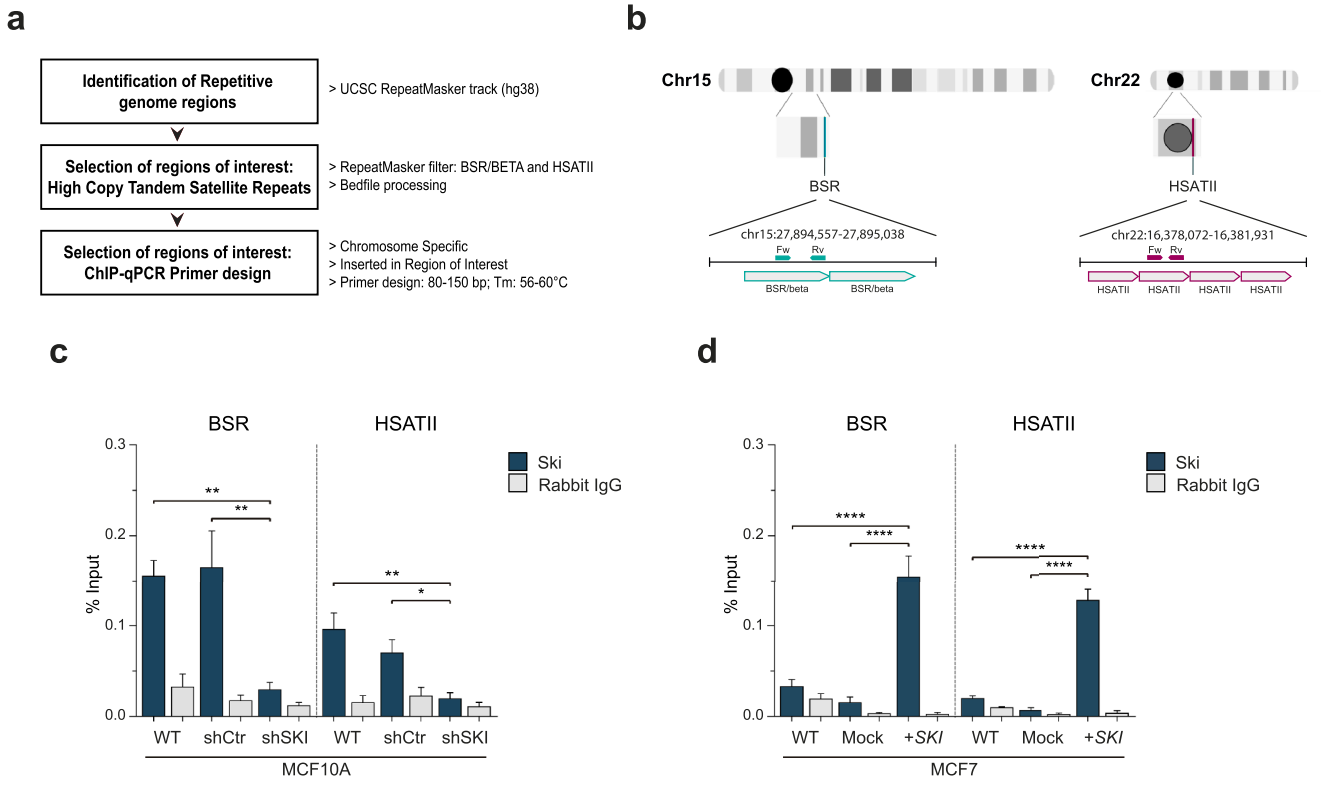

Fig. 3. SKI associates with BSR and HSATII satellite DNA during mitosis. Schematic representation of primer design strategy (a) and locations of primers used for BSR (chromosome 15) and HSATII (chromosome 22) (b). (c-d) SKI occupancy on BSR and HSATII in mitotic MCF10A and MCF7 cells. ChIP enrichment is expressed as % of input ± SEM. Normal IgG served as a specificity control. Statistical significance was determined by one-way ANOVA with multiple comparisons. Significance levels are indicated by asterisks: *p < 0.05, **p < 0.01, ****p < 0.0001.

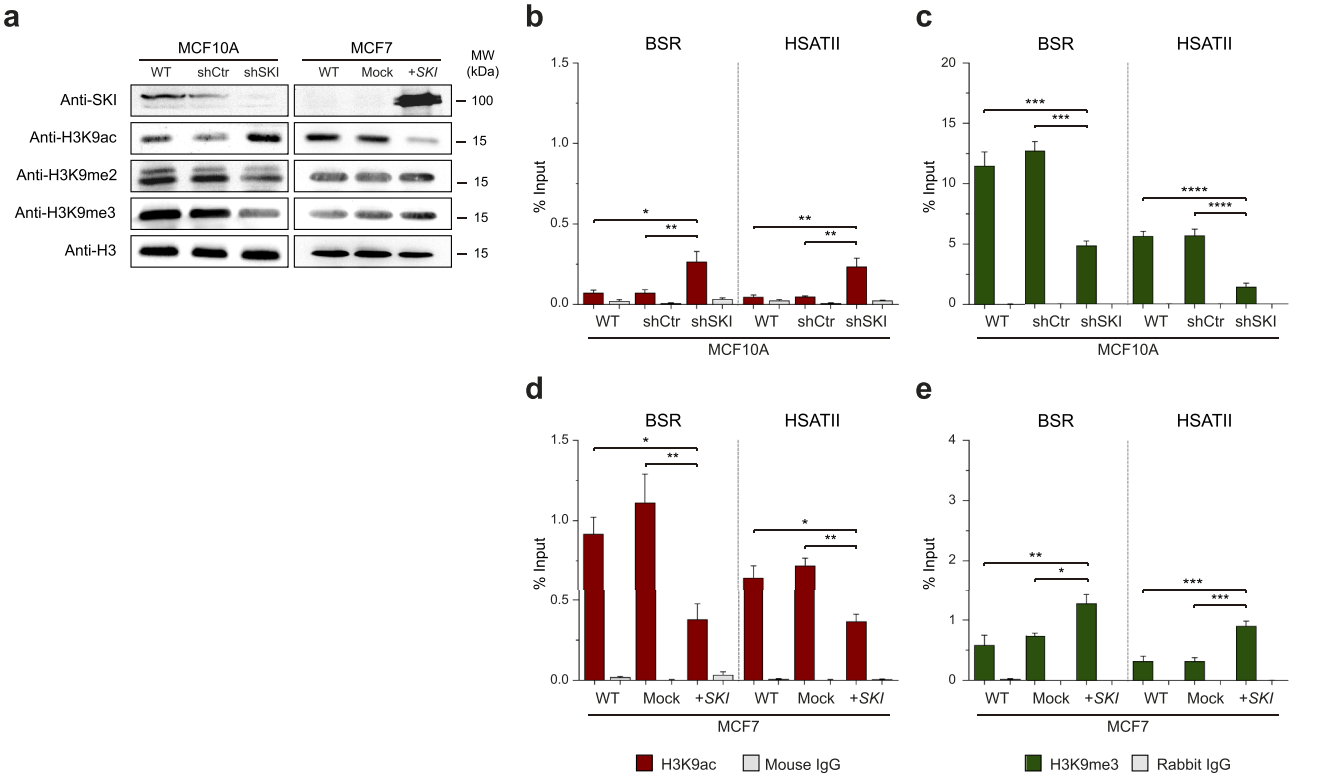

Fig. 4. SKI-dependent heterochromatin H3K9 methylation on BSR and HSATII satellites. (a) SKI and H3K9 modifications levels were assessed by western blotting in MCF10A and MCF7 cells using specific antibodies. Anti-H3 was used as a loading control. (b-e) SKI-dependent H3K9 Acetylation and Methylation at PCH. ChIP assays were performed to assess H3K9 modifications on BSR and HSATII in mitotic MCF10A (b-c) and MCF7 (d-e) cells. ChIP enrichment is expressed as % of input ± SEM. Normal IgG served as a specificity control. Statistical significance was determined by one-way ANOVA with multi-comparisons. Significance levels are indicated by asterisks: *p < 0.05, **p < 0.01, ***p ≤ 0.001, ****p < 0.0001.

chromosomal instability.

Discussion

Proper pericentromeric organization is crucial for accurate chromosome segregation, and disruptions in this region contribute to genomic instability and tumor progression [1]. While previous studies in murine embryonic fibroblasts (MEFs) show that Ski is required for proper chromosome segregation [21] and is localized in mitotic chromosomes [13], its specific localization and function in human cells remained unclear. This study demonstrates a distinct pericentromeric localization of Ski in human mitotic chromosomes, particularly at acrocentric chromosomes. This localization is enriched in non-transformed fibroblasts and MCF10A epithelial cells, while in MCF7, the transformed counterpart, the protein is also found in non-acrocentric chromosomes (Fig. 1). Nevertheless, this could not be confirmed because of these cells' high level of aneuploidy and chromosomal rearrangements. This differential distribution could be related to the cell type (epithelial v.s. fibroblasts) or its transformation status (non-transformed v.s. tumor-derived cell line). This latest explanation would be consistent with the features of the TGFβ signaling in different tissues and cell types. It could also determine whether SKI acted as an oncogene or a tumor suppressor, as described [14].

This localization for SKI in human chromosomes is very intriguing since all mouse chromosomes are acrocentric. Yet, not all of them have this localization pattern, suggesting that binding SKI to chromosomes relies on specific nucleotide sequences, for instance, SMAD-binding elements in the *mmp3* gene promoter [13].

Human acrocentric chromosomes harbor Nucleolus Organization Regions (NORs). Thus, localization of SKI in acrocentric chromosomes was further confirmed by the association of the protein with UBF, a transcription factor for rDNA genes.

Our key findings indicate that SKI manipulation affects H3K9 acetylation and methylation patterns at the rDNA promoter, subsequently impacting 45S rRNA synthesis. Specifically, SKI knockdown resulted in decreased H3K9 methylation and increased H3K9 acetylation, while SKI overexpression led to the opposite effects. These epigenetic changes were associated with alterations in 45S rRNA expression levels, with SKI knockdown increasing and SKI overexpression reducing 45S rRNA synthesis. These results suggest that SKI plays a critical role in the epigenetic regulation of rDNA transcription.

Emerging evidence indicates that transcription factors involved in cell proliferation and growth bind to chromosomes during mitosis and determine the early gene expression in the next cell cycle. Our group has provided evidence to consider Ski as a mitotic bookmarker factor for the *mmp3* gene in MEFs. During mitosis, UBF remains associated with NOR sequences with active rDNA promoters [27–29]. Our data about the mitotic co-localization of SKI with UBF, the reduction of H3K9ac levels in *SKI* overexpression, and the transcriptional difference in rDNA gene expression associated with SKI levels suggest that SKI could be acting as a mitotic bookmark for repression of rDNA genes.

Cancer cells exhibit increased rRNA expression and enlarged nucleoli, both critical for their rapid proliferation. The rate of ribosomal RNA synthesis in the nucleolus is a crucial regulator of cellular proliferation and a potential target for therapeutic intervention in cancer [30, 31]. Understanding the involvement of SKI in rRNA synthesis and silencing mechanisms in transformed cells may lead to new treatment approaches for malignancies.

SKI depletion also leads to reduced H3K9me3 levels and decreased SUV39H1 and HP1α occupancy at BSR and HSATII satellite repeats. Conversely, SKI overexpression enhances H3K9me3 and reduces H3K9 acetylation in these regions. These results indicate that Ski is crucial in

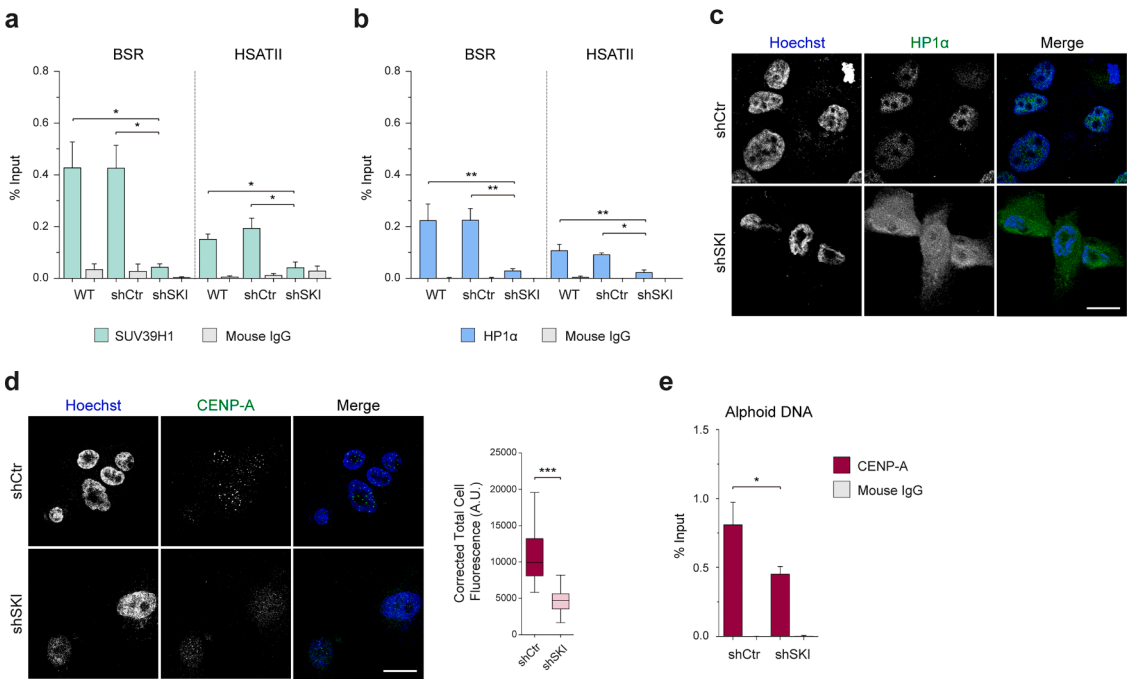

Fig. 5. SKI deficiency disturbs Suv39H1 and HP1α binding to pericentric satellites, and CENP-A loading at centromeres. (a-b) SUV39H1 and Heterochromatin Protein 1A (HP1α) enrichment at pericentric satellites in MCF10A cells. Statistical significance was determined using one-way ANOVA with multi-comparisons. *$p < 0.05$; **$p < 0.01$. (c) HP1α immunodetection, (d) CENP-A immunodetection and quantification in control (shCtrl) and SKI knockdown (shSKI) MCF10A cells. DNA was visualized with Hoechst staining (scale bar = 15 μm). The quantification of CENP-A nuclear signal is shown on the right. Statistical significance was determined by two-tailed t-test. ***$p < 0.001$. (e) CENP-A occupancy at centromeric alpha satellite DNA. ChIP enrichment is expressed as % of input ± SEM. Normal IgG served as a specificity control. Statistical significance was determined by two-tailed t-test. *$p < 0.05$.

regulating the epigenetic landscape of pericentromeric heterochromatin. SKI protein levels increase progressively from G2 to reach a maximum in mitosis [20], the same as the H3K9 trimethylation levels directed by SUV39H enzymes on pericentromeric regions [5]. This data and our results indicate that the effect of SKI might be a critical factor for SUV39H1 and HP1α activities and recruitment. Deacetylation of H3K9 is an initial and essential event allowing subsequent H3K9 methylation [32]. We propose that SKI-dependent deacetylation events at H3K9 not only influence gene expression preserving nuclear silent domains but also are required for H3K9me3 enrichment at the pericentromeric region, repetitive sequences hypermethylation, correct centromere formation, and chromosome segregation. The association of SKI to mitotic chromatin in a complex with Smad2/3 was previously described in TGFβ-stimulated HaCaT cells [33]. Moreover, it was demonstrated the involvement of HDAC activity in maintaining reduced H3K9ac mitotic levels [29], supporting our findings and hypothesis.

We also determined that Ski depletion affects centromere integrity, as evidenced by aberrant CENP-A incorporation. Given that CENP-A loading occurs primarily during G1/S phase, this indicates that Ski-dependent effects are not limited to mitosis. This is supported by extended deletion regions in the genome of Ski-deficient cells, which indicates the involvement of pre-mitotic mechanisms of CIN.

Pericentromeric repetitive DNA hypomethylation and low H3K9me3 enrichment are frequent in breast adenocarcinoma, correlating with chromosomal rearrangements, aberrant satellite DNA overexpression, and aneuploidy [8]. This is consistent with our findings that breast tumors with low levels of Ski expression have significantly higher chromosome instability and aneuploidy (data not shown).

On the other hand, the failure of rDNA chromatin silencing -frequently observed in cancer cells- leads to aberrant homologous recombination among rDNA repeats within sister chromatids, defects in nucleolar architecture, DNA repair, and oncogenesis [34–36].

While the relevance of these changes in cancer is clear, the mechanisms that drive them are poorly defined. The identification of SKI as a key player in the epigenetic silencing of pericentromeric and ribosomal DNA addresses a significant knowledge gap. This discovery enables new research into the connection between transcriptional regulation and genome instability in cancer and presents new possibilities for therapeutic intervention.

Materials and methods

Antibodies. Primary antibodies used in this study: anti-SKI (SCBT, sc-9140), anti-UBF (SCBT, sc-13125), anti-H3 (Abcam, ab1791), anti-H3K9ac (Abcam, ab12179), anti-H3K9me2 (Abcam, ab32521), anti-H3K9me3 (Abcam, ab8898), anti-CENP-A (Abcam, ab13939), anti-SUV39H1 (Abcam, ab12405), anti-HP1α (Abcam, ab77256) and anti-α-tubulin (Sigma, T5168). Control antibodies for ChIP were nonspecific rabbit IgG (SCBT, sc-2027) and mouse IgG (SCBT, sc-2025). Centromeres were detected using CREST antiserum (Antibodies Incorporated). Secondary antibodies for WB studies were anti-rabbit IgG-HRP and anti-mouse IgG-HRP (Bio-Rad). Secondary antibodies for IF studies were Alexa Fluor 488 anti-rabbit IgG(H+L), Alexa Fluor 594 anti-rabbit IgG (H+L), Alexa Fluor 594 anti-mouse IgG(H+L), Alexa Fluor 488 anti-mouse IgG(H+L) and anti-human DyLight 594 (Molecular probes).

Cell culture. MRC-5 and primary fibroblasts were cultured in MEM supplemented with 10 % of inactivated FBS (Gibco) and 2 mM L-glutamine (HyClone). MCF7s were cultured in DMEM (Gibco) supplemented with 10 % of FBS and 50 U/ml penicillin-streptomycin (Gibco). MCF10A cells were cultured in DMEM/F12 (50:50) (HyClone) supplemented with 5 % of Horse Donor Serum (Mediatech), 50 U/ml penicillin-streptomycin, 0.5 μg/ml hydrocortisone (Sigma-Aldrich), 10 ng/ml hEGF (R&D System) and 10 ng/ml insulin (Sigma-Aldrich). All cells were maintained at 37°C and 5 % of CO2 until 70-80 % of confluence.

Cell Synchronization. Cell lines were synchronized using 50 ng/ml colcemid (Sigma-Aldrich) for 16 h. Mitotic cells were obtained by mitotic shake off.

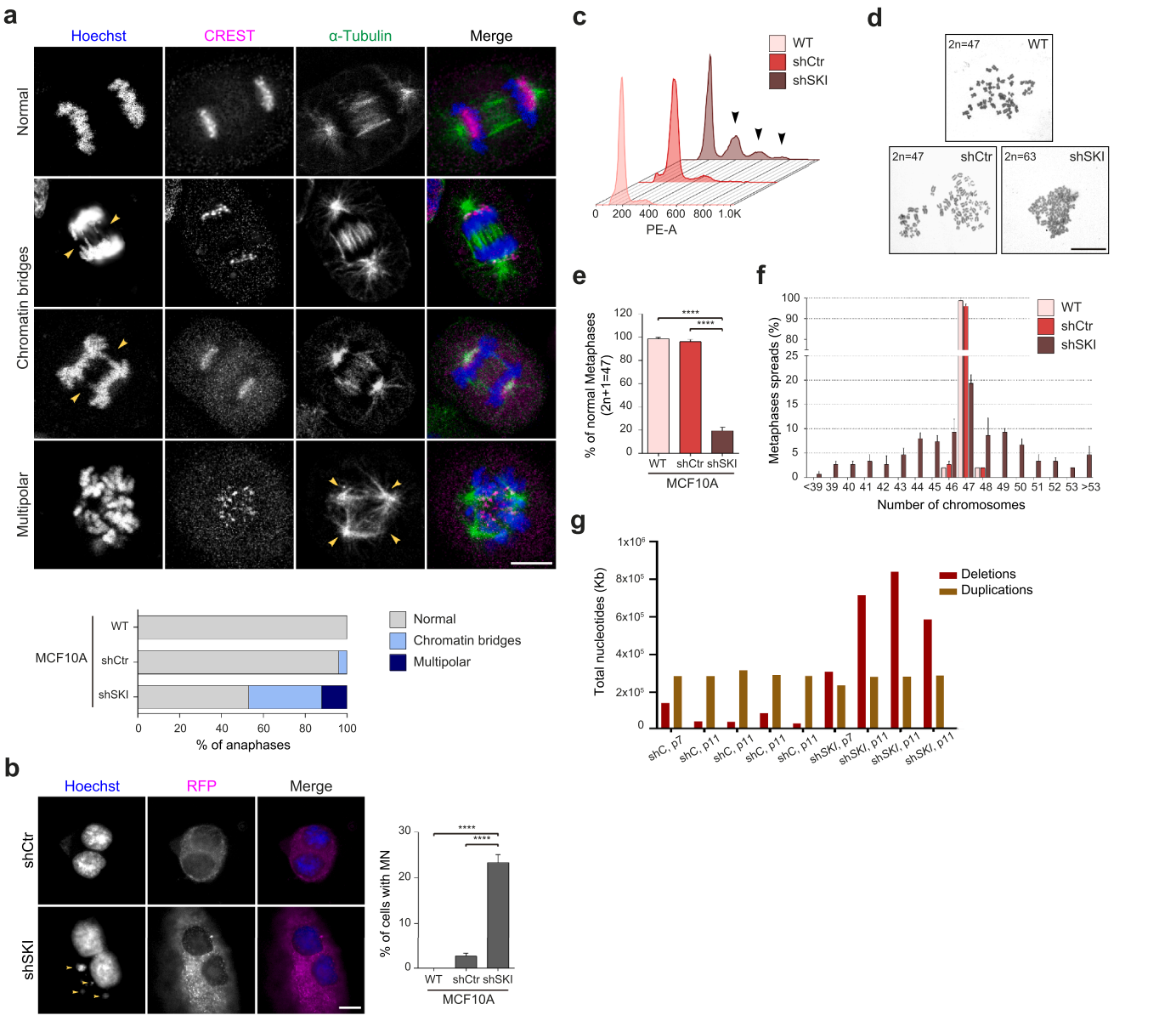

Fig. 6. SKI deficiency induces chromosome instability (CIN). (a) Mitotic aberrations in shSKI MCF10A cells. Representative images show normal anaphases, chromatin bridges (yellow arrows), and multipolar anaphases (yellow arrowheads) in SKI knockdown (shSKI) MCF10A cells. CREST and α-tubulin staining visualize centromeres and spindles, respectively. Scale bar = 4 μm. Quantification of normal and abnormal anaphases is shown at the bottom. (b) Micronucleus formation upon SKI knockdown. Representative images show micronuclei (yellow arrowheads) in control (shCtrl) and SKI knockdown (shSKI) MCF10A cells. Scale bar = 4 μm. RFP= Red Fluorescent Protein. Quantification of the percentage of cells with micronuclei is shown on the right (mean ± SEM). (c-f) Aneuploidy in SKI deficient cells, assessed by DNA content (c, black arrowheads indicate polyploid populations) and metaphase chromosome quantification (d-f). Representative metaphase spreads are shown in panel d (scale bar = 10 μm). Panel (e) quantifies normal metaphases with the expected chromosome number (2n = 47). The average chromosome number per metaphase in WT, shCtrl, and shSKI MCF10A cells is shown in panel f (n = 100 cells per cell line, three independent experiments). Quantification values are expressed as mean ± SEM. Statistical analyses were performed using one-way ANOVA with multiple comparisons. ****p < 0.0001. (g) increased CNV in Ski deficient cells. The extension of deletions and insertions are shown.

Conventional and mitotic spread immunofluorescence (IF). IF assays were performed as previously reported [13]. For conventional IF, MCF10A cells were cultured on nitrocellulose-treated coverslips, fixed in 3.7 % paraformaldehyde for 10 min at room temperature (RT), and quenched with 100 mM glycine for 5 min. Cells were permeabilized with 0.5 % Triton X-100 in PBS for 10 min and blocked in 3 % BSA in PBS for 45 min. Primary antibodies diluted in PBS were incubated overnight, followed by secondary antibodies diluted 1:500 in 1 % BSA, 0.05 % Triton X-100 for 45 min. For mitotic spreads, MCF10A cells were synchronized in M phase, collected by shake-off, and treated with 75 mM KCl for 15 min at 37 °C. Cells were adhered to coverslips via cytocentrifugation and treated with KCM buffer (120 mM KCl, 20 mM NaCl, 10 mM Tris-HCl pH 7.5, 0.5 mM EDTA, 0.1 % Triton X-100) for 5 min. Antibodies were applied as conventional IF but diluted in KCM buffer with 1 % BSA and 0.05 % Triton X-100.

DNA was stained with 1 μg/ml of Hoechst (Invitrogen) for 5 min at RT. Samples were mounted in ProLong™ Gold antifade reagent (Invitrogen) with coverslips, and images were collected by confocal microscopy using an Eclipse Ti (Nikon) and were analyzed using the NIS element software. Selected z-stacks were used to compose figures using ImageJ software.

Chromatin immunoprecipitation (ChIP). ChIP analyses were performed with cross-linked chromatin samples as described previously [13]. Cross-linked chromatin was sheared into fragments of 200-300 bp,

and immunoprecipitation were conducted using specific antibodies targeting histone post-translational modifications and proteins of interest. Immunoprecipitated DNA was purified and quantified by quantitative PCR (qPCR), with enrichment levels calculated as a percentage of the input chromatin. *SMAD7* promoter was used as positive control for SKI (Fig. S1).

Design of chromosome-specific primers for qPCR

Regions of interest were selected based on high-copy tandem satellite repeats by applying the UCSC RepeatMasker track (hg38), specifically targeting BSR/BETA and HSATII, followed by bedfile processing. Finally, regions of interest are further refined for ChIP-qPCR primer design. The primers are chromosome-specific, inserted within the region of interest, and designed to be 80–150 bp in length with a melting temperature (Tm) of 56–60°C (**Table S1**)

Immunoblotting. Purified histones were obtained using a standard acid extraction method [37]. Cell lysates were prepared in RIPA buffer supplemented with a protease (Calbiochem) and phosphatase (Roche) inhibitor cocktail, according to the manufacturer's instructions. Bradford's assay quantified protein levels.

For Immunoblot analyses, 2 µg of purified histones and 30 µg of total cell lysis were subjected to SDS-PAGE and transferred to a PVDF membrane. All primary antibodies were incubated at 4°C overnight and detected using appropriate HRP-conjugated secondary antibodies and chemiluminescence reagent (Millipore). Images were obtained using the ChemiScope3500 (Clinx Science Instruments).

Micronucleus assay. All MCF10A cells were cultured in 110-mm-diameter cover glass with 18-mm coverslips. When the cells reached 70 % confluence, 6 µg/ml Cytochalasin B was added and incubated overnight at 37°C and 5 % CO2. Then, conventional IF was performed as described before.

Plasmids, transfection, and transduction. MCF7 cells were transfected with RIGB-T7-SKI [15] or empty vector using Lipofectamine™ 3000 Reagent (Invitrogen) and selected for resistance to 10 µg/ml Blasticidin (Gibco) for 72 h, followed by Fluorescence-activated cell sorting (FACS) of GFP+ cells.

SKI-specific and scramble shRNAs were obtained using GenTarget́s designer software (**Table S2**). shRNA hairpins were cloned into GenTarget's lentiviral shRNA expression vector expressing RFP-puromycin. MCF10A cells were transduced with lentiviral particles (MOI:5) on DMEM/F12 supplemented with 5 µg/ml polybrene for 48 h. shSKI #1, shSKI #2, and shCtr MCF10As were selected by resistance to 0.5 ug/ml puromycin (Gibco) for 72 h, and RFP expression by FACS.

RT-qPCR analysis. Total RNA was performed using TRIzol (Thermo Fisher Scientific) according to the supplieŕs instructions. 1 µg RNA was reverse-transcribed using the AffinityScript qRT-PCR cDNA Synthesis Kit (Agilent Technologies). RT-qPCR was performed by using Brilliant II SYBR green qPCR master mix (Agilent Technologies) in an Eco Real-Time PCR System (Illumina). Analysis was performed by ΔΔCt method. *HPRT1* expression was used as housekeeping gene. Primers used are listed in **Table S3**.

Whole-Exome Sequencing. gDNA was purified from MCF10 shCtrl and shSKI from different batches and passage numbers. 1ug was submitted to Novogene Co. Ltd. for whole exome sequencing using Agilent v6 library and 150 × 2 pair-end sequencing in Illumina Novaseq equipment (6Gb). Bioinformatic analysis followed in the Seven Bridges platform, using GATK best practices for pre-processing and CNVkit for copy number analysis. GRCh37/hg19 genome was used as reference.

Statistical Analysis. RT-qPCR, ChIP, chromosome number, and MN assays were examined by Student's t-test with Welch correction or One/Two Way ANOVA with Bonferroni post-test, as depicted in the legend of each figure. $P < 0.05$ was considered statistically significant. At least three independent experiments were performed for each analysis. Statistical analysis was performed using PRISM 9.0 (GraphPad Software).

For quantitative fluorescence image analysis, nuclei were analyzed using ImageJ software.

Funding sources

This work was supported by ANID Grants FONDECYT 1221162, 1151435, 1211026, 1151435, Millennium NCN2023_032, ACT210079 & FONDAP 152220002 (CECAN).

Funding sources had no involvement in the study design, collection, analysis and interpretation of data, writing of the report and decision to submit the article for publication.

Declaration of generative AI and AI-assisted technologies in the writing process

While preparing this work the author(s) used Grammarly and Gemini Advance 2.0 to improve the readability and language of the manuscript. After using this tool/service, the author(s) reviewed and edited the content as needed and take(s) full responsibility for the content of the published article.

CRediT authorship contribution statement

Víctor Pola-Véliz: Conceptualization, Methodology, Investigation, Writing – original draft, Formal analysis. **David Carrero:** Investigation, Writing – original draft, Formal analysis, Methodology. **Eduardo A. Sagredo:** Formal analysis, Investigation, Methodology. **Víctor Inostroza:** Investigation, Methodology, Formal analysis. **Claudio Cappelli:** Conceptualization, Writing – original draft, Investigation. **Solange Rivas:** Methodology, Investigation, Formal analysis. **Mirit Bitrán:** Investigation, Methodology, Formal analysis. **Evelyn Zambrano:** Data curation, Formal analysis, Investigation. **Evelin Gonzalez:** Data curation, Formal analysis. **Fernanda Morales:** Validation, Writing – review & editing. **Marcia Manterola:** Supervision, Writing – review & editing. **Martín Montecino:** Writing – review & editing, Supervision, Resources. **Ricardo Armisén:** Writing – review & editing, Funding acquisition. **Katherine Marcelain:** Supervision, Formal analysis, Writing – original draft, Funding acquisition, Conceptualization.

Declaration of competing interest

The authors declare that they have no known competing financial interests or personal relationships that could have appeared to influence the work reported in this paper.

Acknowledgements

The authors thank B. Pesce, PhD, for supporting flow cytometric and cell sorting procedures at the MED.UCHILE-FACS Facility (FONDEQUIP140032 (BD LSR Fortessa X-20, Special Order) and AIC-08 (BD FACSAria III). Dr. Manuel Meruane for his support on cell culturing.

Supplementary materials

Supplementary material associated with this article can be found, in the online version, at doi:10.1016/j.neo.2025.101204.

References

[1] S.O. Siri, J. Martino, V. Gottifredi, Structural chromosome instability: types, origins, consequences, and therapeutic opportunities, Cancers 13 (2021) 3056.
[2] T. Fukagawa, WC. Earnshaw, The centromere: chromatin foundation for the kinetochore machinery, Dev. Cell 30 (2014) 496–508.
[3] O. Vafa, KF. Sullivan, Chromatin containing CENP-A and α-satellite DNA is a major component of the inner kinetochore plate, Curr. Biol. 7 (2004) 897–900.
[4] L.L. Sullivan, K. Chew, BA. Sullivan, a satellite DNA variation and function of the human centromere, Nucleus. 8 (2017) 331–339.
[5] C. Maison, G. Almouzni, HP1 and the dynamics of heterochromatin maintenance, Nat. Rev. Mol. Cell Biol. 5 (2004) 296–304.

[6] A.B. Sharma, S. Dimitrov, A. Hamiche, E. Van Dyck, Centromeric and ectopic assembly of CENP-A chromatin in health and cancer: old marks and new tracks, Nucleic. Acids. Res. 47 (2019) 1051–1069.
[7] N. Saksouk, E. Simboeck, J. Déjardin, Constitutive heterochromatin formation and transcription in mammals, Epigenetics. Chromatin. 8 (2015) 1–17.
[8] F. Bersani, E. Lee, P.V. Kharchenko, A.W. Xu, M. Liu, K. Xega, et al., Pericentromeric satellite repeat expansions through RNA-derived DNA intermediates in cancer, Proc. Natl. Acad Sci. 112 (2015) 15148–15153.
[9] J.S. Verdaasdonk, K. Bloom, Centromeres: Unique chromatin structures that drive chromosome segregation, Nat. Rev. Mol. Cell Biol. 12 (2011) 320–332.
[10] S. Machida, Y. Takizawa, M. Ishimaru, Y. Sugita, S. Sekine, J. Nakayama, et al., Structural basis of heterochromatin formation by human HP1, Mol. Cell 69 (2018) 385–397.e8.
[11] S. Weirich, M.S. Khella, Jeltsch A. Structure, Activity and Function of the Suv39h1 and Suv39h2 protein lysine methyltransferases, Life 11 (2021) 703.
[12] S. Fioriniello, D. Marano, F. Fiorillo, M. D'Esposito, F. Della Ragione, Epigenetic factors that control pericentric heterochromatin organization in mammals, Genes 11 (2020) 595.
[13] C. Cappelli, H. Sepulveda, S. Rivas, V. Pola, U. Urzúa, G. Donoso, et al., Ski is required for Tri-methylation of H3K9 in major satellite and for repression of pericentromeric genes: Mmp3, Mmp10 and Mmp13, in mouse fibroblasts, J. Mol. Biol. 432 (2020) 3222–3238.
[14] C. Bonnon, Atanasoski S. c-Ski in health and disease, Cell Tissue Res. 347 (2012) 51–64.
[15] N. Ueki, MJ. Hayman, Direct interaction of Ski with either Smad3 or Smad4 is necessary and sufficient for Ski-mediated repression of transforming growth factor-β signaling, J. Biol. Chem. 278 (2003) 32489–32492.
[16] C. Feld, P. Sahu, M. Frech, F. Finkernagel, A. Nist, T. Stiewe, et al., Combined cistrome and transcriptome analysis of SKI in AML cells identifies SKI as a co-repressor for RUNX1, Nucleic. Acids. Res. 46 (2018) 3412–3428.
[17] B.T. Vo, B. Cody, Y. Cao, SA. Khan, Differential role of Sloan-Kettering Institute (Ski) protein in nodal and transforming growth factor-beta (TGF-β)-induced smad signaling in prostate cancer cells, Carcinogenesis 33 (2012) 2054–2064.
[18] I Theohari, I Giannopoulou, C Magkou, A Nomikos, S Melissaris, L Nakopoulou, Differential effect of the expression of TGF-β pathway inhibitors, Smad-7 and Ski, on invasive breast carcinomas: relation to biologic behavior, APMIS 120 (2012) 92–100.
[19] Rivas S, Armisén R, Rojas DA, Maldonado E, Huerta H, Tapia JC, Espinoza J, Colombo A, Michea L, Hayman MJ, Marcelain K. The Ski Protein is Involved in the Transformation Pathway of Aurora Kinase A. J Cell Biochem. 2016 Feb;117(2): 334-43. doi: 10.1002/jcb.25275. PMID: 26138431.
[20] K. Marcelain, MJ. Hayman, The Ski oncoprotein is upregulated and localized at the centrosomes and mitotic spindle during mitosis, Oncogene 24 (2005) 4321–4329.
[21] K. Marcelain, R. Armisen, A. Aguirre, N. Ueki, J. Toro, C. Colmenares, et al., Chromosomal instability in mouse embryonic fibroblasts null for the transcriptional co-repressor Ski, J. Cell Physiol. 227 (2011) 278–287.
[22] H. Tsuda, T. Takarabe, Y. Kanai, T. Fukutomi, S. Hirohashi, Correlation of DNA hypomethylation at pericentromeric heterochromatin regions of chromosomes 16 and 1 with histological features and chromosomal abnormalities of human breast carcinomas, Am. J. Pathol. 161 (2002) 859–866.
[23] B. Schuster-Böckler, B. Lehner, Chromatin organization is a major influence on regional mutation rates in human cancer cells, Nature 488 (2012) 504–507.
[24] A. Narayan, J.I. Weizhen, X. Zhang, A. Marrogi, J.R. Graff, S.B. Baylin, et al., Hypomethylation Of pericentromeric DNA in breast adenocarcinomas, Int. J. Cancer 77 (1998) 833–838.
[25] A. Eymery, B. Horard, M.E. Atifi-Borel, G. Fourel, F. Berger, A-L Vitte, et al., A transcriptomic analysis of human centromeric and pericentric sequences in normal and tumor cells, Nucleic. Acids. Res. 37 (2009) 6340–6354.
[26] R. Slee, C. Steiner, B-S Herbert, G. Vance, R. Hickey, T. Schwarz, et al., Cancer-associated alteration of pericentromeric heterochromatin may contribute to chromosome instability, Oncogene 31 (2011) 3244–3253.
[27] R. Srivastava, R. Srivastava, SH. Ahn, The Epigenetic Pathways to Ribosomal DNA Silencing, Microbiol. Mol. Biol. Rev. 80 (2016) 545–563.
[28] P. Roussel, C. Andr, L. Comai, D. Hernandez-verdun, I.J. Monod, P. Cedex, et al., The rDNA transcription machinery is assembled during mitosis in active NORs and absent in inactive NORs, J. Cell Biol. 133 (1996) 235–246.
[29] M.V. Sluis, C.V. Vuuren, H. Mangan, B. Mcstay, NORs on human acrocentric chromosome p-arms are active by default and can associate with nucleoli independently of rDNA, Proc. Natl. Acad Sci. U A 117 (2020) 10368–10377.
[30] L.X.T. Nguyen, A. Raval, J.S. Garcia, BS. Mitchell, Regulation of ribosomal gene expression in cancer, J. Cell Physiol. 230 (2015) 1181–1188.
[31] M. Long, X. Sun, W. Shi, A. Yanru, S.T.C. Leung, D. Ding, et al., A novel histone H4 variant H4G regulates rDNA transcription in breast cancer, Nucleic. Acids. Res. 47 (2019) 8399–8409.
[32] D. Nicetto, KS. Zaret, Role of H3K9me3 heterochromatin in cell identity establishment and maintenance, Curr. Opin. Genet. Dev. 55 (2019) 1–10.
[33] S. Gandhi, R. Mitterhoff, R. Rapoport, M. Farago, A. Greenberg, L. Hodge, et al., Mitotic H3K9ac is controlled by phase-specific activity of HDAC2, HDAC3, and SIRT1, Life Sci. Alliance 5 (2022) e202201433.
[34] T. Tabata, K. Kokura, P. ren Dijke, S. Ishii, Ski co-repressor complexes maintain the basal repressed state of the TGF-β target gene, SMAD7, via HDAC3 and PRMT5, Genes. Cells 14 (2009) 17–28.
[35] D.O. Warmerdam, RMF. Wolthuis, Keeping ribosomal DNA intact: a repeating challenge, Chromosome Res. 27 (2019) 57–72.
[36] E. Smirnov, N. Chmúrčiaková, D. Cmarko, Human rDNA and Cancer, Cells 10 (2021) 3452.
[37] D. Shechter, H.L. Dormann, C.D. Allis, SB. Hake, Extraction, purification and analysis of histones, Nat. Protoc. 2 (2007) 1445–1457.